Tanzania Journal of Science 46(2): 534-547, 2020
ISSN 0856-1761, e-ISSN 2507-7961
© College of Natural and Applied Sciences, University of Dar es Salaam, 2020

Preparation and Characterization of ZnS Thin Films Grown by Spin Coating Technique

Oluwatoyin Osanyinlusi
Department of Physics, University of Ilorin, Ilorin, Kwara State, Nigeria
E mail: adetolusi@gmail.com

Received 6 May 2020, Revised 18 June 2020, Accepted 25 June 2020, Published June 2020

Abstract

Spin coating technique was used to deposit zinc sulphide (ZnS) thin films successfully onto glass substrates and the effects of the number of spin times on the optical properties investigated. The morphology and structures of the prepared thin films were also confirmed. X-ray diffraction confirmed that spin coated ZnS films exhibited cubic structure, where reflections from (111), (220) and (311) are clearly visible with a preferential orientation along (111) plane. The calculated crystallite size for 1S sample from the XRD data is 8.8 nm. From the optical studies, the thin films exhibit good optical properties with relatively high transmittance (81 %) and low absorbance in the visible region. The transmittance decreases as the number of spin time increases, and this may be attributed to increase in thickness of the films. This feature is reflected in all the other optical parameters. The band gaps obtained ranged from 3.70 to 3.87 eV, which are relatively higher than the energy band gap of the bulk ZnS material (i.e., 3.65 eV) and it increases with increasing number of spin times. The SEM micrograph showed that the films deposited are uniform throughout the surface without voids. EDX analysis showed the presence of zinc and sulphur in the prepared films with percentages by weights of 78.2% and 6.0%, respectively, showing that the films are sulphur deficient. These results therefore showed that the prepared ZnS films exhibit properties of materials that can be used as optoelectronic devices especially as window for photovoltaic cells.

Keywords: Zinc sulphide thin films, Spin coating technique, Optoelectronic properties, EDX, Surface morphology.

Introduction

Recent studies on solar cells fabrication are geared towards reducing the fabrication costs in order to lower the price of the energy obtained. As such, the studies are directed at making use of thin films technology for their fabrication (Nair 1998). Due to the crucial role of zinc sulphide (ZnS) thin films in optoelectronic and photovoltaic devices, scientists and researchers have given more attention to the study of the properties of this compound. Generally, ZnS crystals exist in two forms; cubic (zinc blende) and hexagonal (wurtzite). The cubic form is stable at room temperature, while wurtzite, the less dense hexagonal form is stable at high temperature (>1020 °C) at atmospheric pressure (Arandhara et al. 2015, Berger 1997, Eid et al. 2010). ZnS is a group II–VI n-type semiconducting material with a wide direct band gap of 3.65 eV (Gao et al. 2004), wide wavelength passband (Arandhara et al. 2015), high refractive index (2·35 at 632 nm) and dielectric constant (Ortíz-Ramos et al. 2014,

Rahchamani et al. 2015). The optical properties make it useful as a filter, reflector and planar wave guide (Mach and Müller 1982).

Although CdS is one of the most promising buffer layer for thin film heterojunction solar cells, ZnS has a wider energy band gap and when used to replace CdS, it results in the transmission of more high-energy photons to the junction, thereby enhancing blue response of photovoltaic cells (Nasr et al. 2006). Furthermore, the use of CdS thin films in large scale solar cell production could cause environmental problems due to high amount of waste from Cd compounds (Johnston et al. 2002, Sartale et al. 2005). Therefore, search for a Cd-free buffer layer materials have become a subject of interest and efforts geared towards overcoming these problems are still ongoing (Khatri and Patel 2018, Choudapura et al. 2019). Thin films of ZnS have been successfully used as buffer layers to replace the CdS in CIGS based solar cells and have achieved a maximum efficiency of 18.6% (Liu et al. 2014).

ZnS thin film is mostly suitable as a window layer in heterojunction photovoltaic solar cells; because the wide band gap reduces the window absorption losses and improves the short circuit current of the cell (Kumar et al. 2015). Researches have shown that ZnS is transparent to visible light, opaque to ultraviolet radiation and near infra-red radiations (Osiele 2001). ZnS materials could also be used in radio frequency field spattered films such as CdZnS and modified ZnS/CdS (Oladeji and Chow 2005).

Different techniques have been used to fabricate ZnS thin films, like sputtering (Shao et al. 2003), molecular beam epitaxy (Kavanagh and Cameron 2001), spray pyrolysis (Elidrissi et al. 2001), successive ionic layer adsorption and reaction technique (Nicolau 1985), pulsed-laser deposition (Yano et al. 2003), chemical bath deposition (Fukarova-Juruskovska et al. 1997), chemical vapour deposition (Kashani 1996), liquid phase atomic layer expitaxy (Lindroos et al. 1994) and spin coating (Kumar et al. 2015). Among these, the spin coating techniques is an attractive method for thin film deposition for various reasons: it is less hazardous, less costly, progressively more uniform as it thins, fast operating system and thus capable of easy scaling up. Additionally, the growth of the films occurs at a relatively low temperature, compatible with flexible organic substrates. As such, there is no need for the use of metal catalysts, and thus it can be integrated with well-developed silicon technologies. Also, there are varieties of parameters (spin speed, time of spin, acceleration, fume exhaust, etc.) that can be adjusted to effectively control the morphologies and properties of the final product (Tyona 2013).

In this study, focus is on the deposition of good quality ZnS thin films by spin coating method. ZnS thin film samples were prepared at different number of spin times, for a maximum of up to four spin times. The resulting ZnS thin films were characterized by X- ray diffraction, scanning electron microscopy (SEM) and UV-Vis spectrophotometer. These characterizations were used to determine the structural, morphological, and optical properties of the films, respectively in order to ascertain the effects of coating spin times on the optoelectronic properties of the materials.

Materials and Methods

Spin coating technique was used to deposit ZnS thin films onto glass substrates by following the procedure described in literature (Balachander et al. 2016). Zinc acetate ($ZnC_4H_6O_4$) was used as zinc ion source and thiourea (CH_4N_2S) as sulphur ion source. 1 M of zinc acetate solution was added to 1 M of thiourea solution using 80% isopropanol and 20% distilled water as solvents. Commercially available glass microscopic slides of dimensions 25.4 mm x 76.2 mm x 1.2 mm were used as substrates. All chemicals were purchased from Sigma Aldrich and were of analytical grade, and the materials were used

as received without any further purification. The solutions were mixed at temperature of 70 °C for 1 hour using a magnetic stirrer coupled with a hot plate. The substrates were cleaned with isopropanol, acetone, and distilled water successively. All the cleanings were done ultrasonically. ZnS thin films were prepared by dropping the prepared solution onto the glass substrate mounted on the spin coater stuck. The spin coater was rotated at1000 rpm for 30 seconds. After each coating, the films were baked inside an oven at 100 °C for 60 minutes, to evaporate the solvent and organic residuals. After that, they were allowed to cool to room temperature inside the oven before applying a new coating. This procedure was repeated for a maximum of four times. Four sets of ZnS thin films were prepared, i.e., one-time spin, two-time spin, three-time spin and four-time spin and were labeled 1S, 2S, 3S and 4S, respectively, giving four sets of samples.

The films were studied for their optical, structural and morphological properties. The optical studies were carried out using Avantes-SAI-07086751 model UV-Vis spectrophotometer in the range of 300 nm to 1000 nm. The spectral data were used to determine the extinction coefficient, refractive index, skin depth, dielectric constants and the band gap of the films. The crystal structure was studied using a Rigaku D/Max–lllC X-ray diffractometer at scanning rate of 2°/min in the range of 10–100° at room temperature with a CuKα radiation of wavelength 1.5406 Å set at 40 kV and 20 mA. Morphological studies of the films were done using a field emission scanning electron microscope (JEOL JSM 7600F Field emission SEM) coupled with an energy dispersion X-ray (EDX) spectrometer to confirm the elemental compositions of the films.

Results and Discussion

Structural analysis

XRD analyses were carried out to investigate the structural properties of the prepared films. Figure 1 shows the XRD pattern of the spin coated ZnS thin film samples obtained at one-time spin (1S). Three intense broadened diffraction peaks can be observed, located at 2θ values of 29.47^{o}, 48.63^{o}, and 57.86^{o}, indexed as (111), (220) and (311). However, the most prominent peak corresponds to the reflections of cubic ZnS with major deviation along (111) direction. The observed XRD pattern is in good agreement with standard data JCPDS reference file No: 05-0566 (Nabiyouni et al. 2011). This observation is similar to previously reported work for ZnS thin film deposited by spin coating technique (Choudapura et al. 2019) and chemical bath deposition (CBD) method (Eid et al. 2010, Tec-Yam et al. 2012). The XRD peaks are broadened due to nanocrystalline nature of samples. As the full width at half maximum intensity (FWHM) increases, the crystallite size decreases and vice versa (Banerjee et al. 2000).

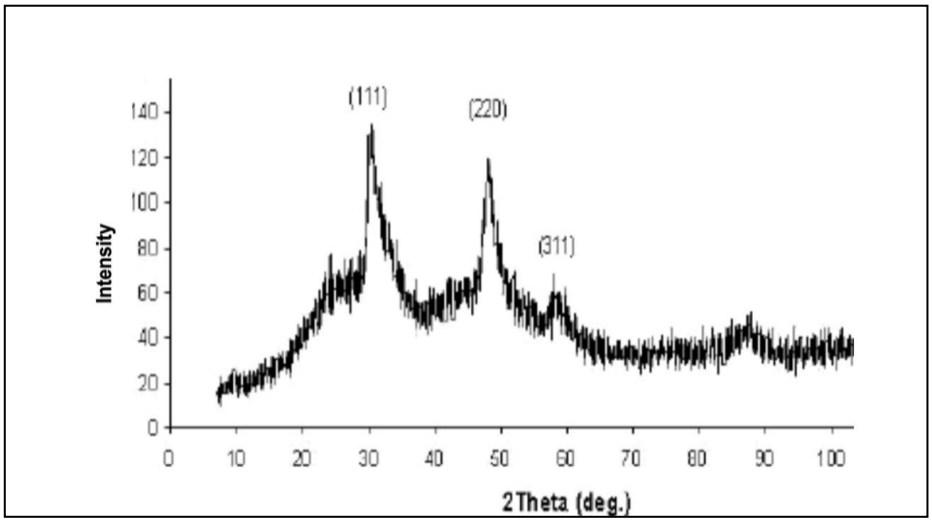


Figure 1: XRD pattern of one- time spin ZnS thin film (sample 1S).

The XRD data were used to determine the crystallite size (*D*), dislocation density (δ) and micro strain (ε) of the (111) diffraction plane. The crystallite size was calculated using Debye-Scherer formula (Bendjedidi et al. 2015);

$$D = \frac{K\,\lambda}{\beta\,Cos\theta} \qquad (1)$$

where: *k* is approximately equal to 0.94, λ is the wavelength of X ray (1.5406 Å), β is the width of the most intense peak at half maximum intensity (0.0169 rad) and θ is the diffraction angle.

A dislocation is a crystallographic defect, or irregularity within a crystal structure. The presence of dislocations (δ) strongly influences many of the properties of materials (Ali 2015). The dislocation density was calculated by the relation (Senthilarasu et al. 2004):

$$\delta = \frac{1}{D^2} \qquad (2)$$

where: *D* is the crystallite size.

The micro strain ε in the film was determined using the relation (Akl et al. 2018):

$$\varepsilon = \frac{\beta\,Cos\theta}{4} \qquad (3)$$

The calculated value of the crystallite size, dislocation density, and micro strain are 8.8 nm, 12.9 x 10^{15} line/m^2 and 4.09 $\times 10^{-3}$, respectively. Nabiyouni et al. (2011) has reported a crystallite size of 8 nm for ZnS thin film deposited by chemical bath method.

Surface morphology

Figures 2 (a) and (b) show the surface morphology of ZnS thin films (1S) deposited at room temperature at different magnifications of 6000x and 8000x as obtained by SEM. From the micrographs, it is observed that the deposited film is uniform throughout the entire surface. The film is without any void or cracks and it covers the substrate well. From the figures, it is observed that there are agglomerations of the small grains.

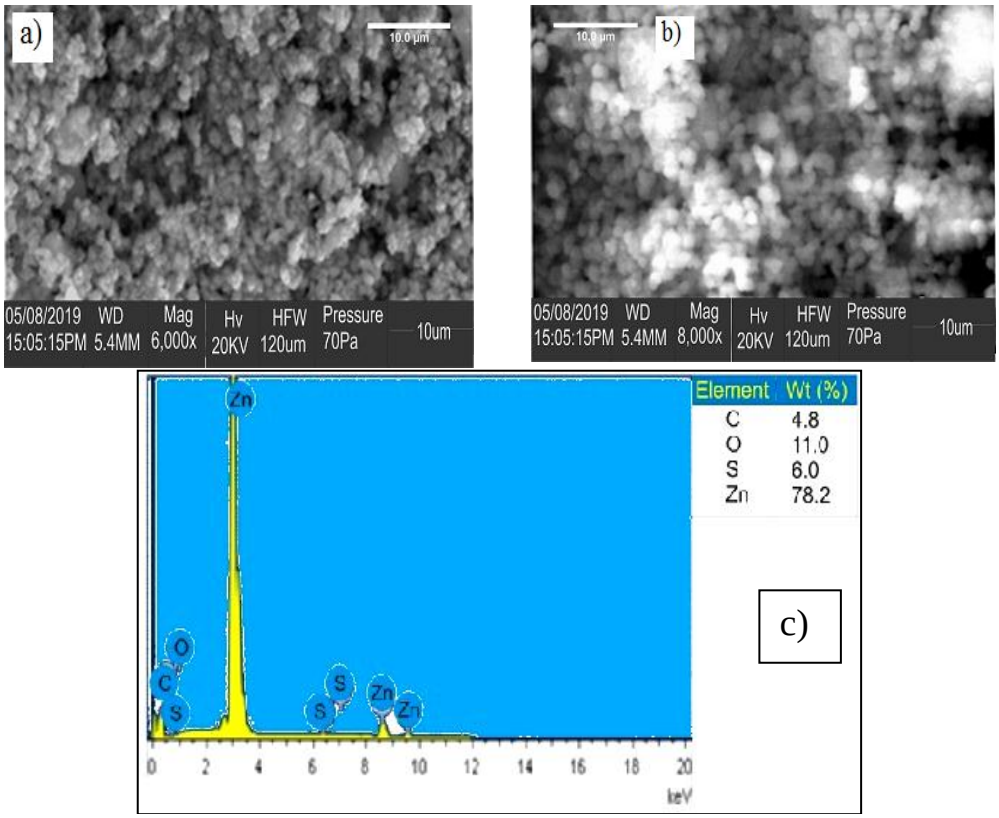


Figure 2: SEM image for 1S at magnifications of (a) 6000x (b) 8000x and (c) EDX for 1S.

Elemental analysis

In order to identify the constituents of the prepared samples, typical EDX analysis was conducted for as-prepared ZnS thin film prepared at one-time spin (1S). The energy dispersive X-ray (EDX) analysis (Figure 2-c) confirms the presence of zinc (Zn) and sulphur (S) in the deposited film. The percentage by weight of zinc and sulphur are 78.2% and 6.0%, respectively. This ratio indicates sulphur deficiency in the film. This may be ascribed to the higher sulphur affinity towards oxygen, so it might have been converted to SO_2 and then evaporated. This is confirmed by the existence of the strong O (oxygen) signal (Shaban et al. 2015). The EDX spectrum also shows the peaks of C (carbon). The presence of O and C may originate respectively from the surrounding air atmosphere and the non-reactive metal salts (Choudapura et al. 2019).

Optical properties

Figures 3 (a, b and c) show the transmittance, absorption and reflectance spectra in the spectra range of 300 to 1000 nm for the ZnS film samples of 1S, 2S and 3S and 4S, respectively. From the transmittance spectra, the highest transmissions observed within the visible region of the spectrum for the 1S, 2S, and 4S samples are 81, 70, and 53%, respectively. The 3S sample shows the same value of highest transmittance of 70% as the 2S film sample. The observed value compares favourably with reported value for ZnS thin films prepared by different methods (Rahimzadeh et al.2018, Erken et al. 2017). It is very important for the buffer layer of a solar cell to be transparent enough in order to allow

the passage of light through to the absorber layer (Bashar et al.2020). These properties show that the ZnS thin film obtained in this study is suitable for use as buffer layer for thin-film solar cells.

It is evident from Figure 3(a) that the transmittance decreases with increasing number of spin times. The observation could be ascribed to increase in the thickness of the films as the number of spin time increases. A sharp rise can also be observed at wavelength < 340 nm for all the films. This may be due to strong absorption of the films in this region as confirmed by the absorption spectra.

The transmission data was used to calculate absorbance (% A) of the films at different wavelengths using the relation (Roy et al. 2006):

$$A = 2 - \log_{10} T \qquad (4)$$

where: T is the percentage transmittance (% T).

The optical absorption spectra of the samples were recorded in the wavelength range between 300 and 1000 nm as presented in Figure 3b. Maximum absorption is observed in the short wavelength region; that is, in the ultraviolet region, for all the ZnS samples and then decreases with increasing wavelength. The overall absorption of the films within the visible region is low (close to zero) and it remains constant at this value throughout the region. It is observed from the plot that the four-time spin has the highest absorbance of 0.36% as compared to the one-time spin which has a low absorbance of 0.20% in the visible region. The increase in absorption due to an increase in number of spins of the films strongly affirms that the optical properties of the films are thickness dependent (Dissanayake and Samarasekara 2018). This is because increase in film thickness implies there are more atoms present, and as such, more states will be available for the photons to be absorbed (Dissanayake and Samarasekara 2018).

The percentage reflectance (%R) is determined from the relation (Abduljabbar 2014):

$$T + A + R = 100 \qquad (5)$$

where: A is the Absorbance (%A), T is the transmittance (%T) and R is the reflectance (%R).

The plot of reflectance against wavelength is presented in Figure 3(c). It is observed that the reflectance decreases with increasing wavelength, but increases with increasing number of spin time with a maximum reflectance of 57% and a minimum reflectance of 21% corresponding to the 4S and 1S film samples, respectively.

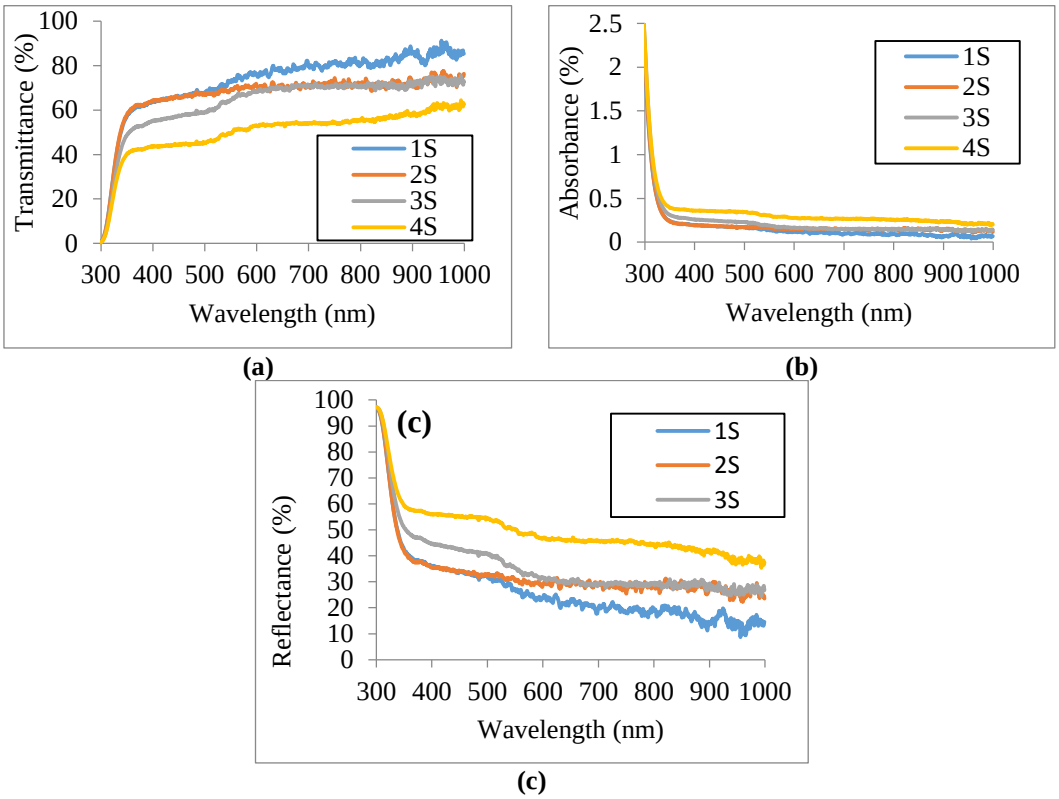


Figure 3: (a) Transmission (b) Absorption and (c) Reflection spectra for 1S, 2S, 3S and 4S.

The extinction coefficient (k) which is directly related to the absorption of photons is calculated from the following equation (Chabou et al. 2019):

$$k = \frac{\propto \lambda}{4\pi} \qquad (6)$$

where: λ is the wavelength of the incident radiation.

Figure 4 shows the variations of extinction coefficient with wavelength for 1S, 2S, 3S and 4S thin films. It is observed that the extinction coefficient spectra follow the same trend as the absorption spectra. The extinction coefficient decreases as the wavelength increases up to 340 nm, and remains constant beyond this value. It is also clear that the extinction coefficient decreases with increasing number of spin time. The sharp increase observed at wavelength <340 nm can be attributed to the strong absorption of ZnS in this region. This behaviour compares favourably with the work of Abduljabbar (2014).

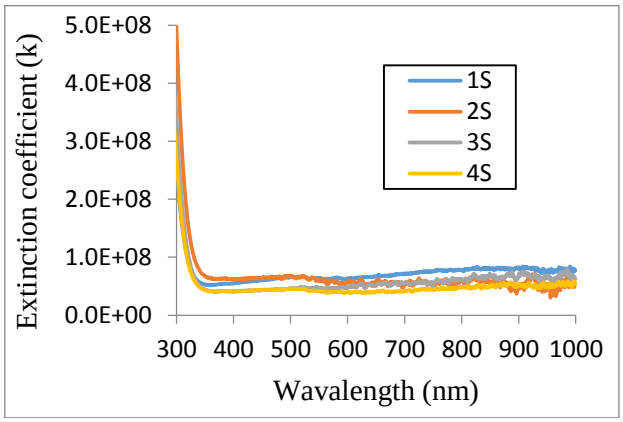


Figure 4: Plot of extinction coefficient against wavelength for 1S, 2S, 3S and 4S.

Refractive index (n) was determined from the reflectance data using the relation (Abdullah et al. 2015);

$$n = \frac{(1 + R^{1/2})}{(1 - R^{1/2})} \qquad (7)$$

where: R is the reflectance (%R).

The variations of refractive index with wavelength for 1S, 2S, 3S and 4S samples in the wavelength range of 300 to 1000 nm are shown in Figure 5. From the figure, it is observed that the refractive index values decrease with increasing number of spins and has a maximum value of 1.23% and a minimum value of 1.09% for 1S and 4S films, respectively.

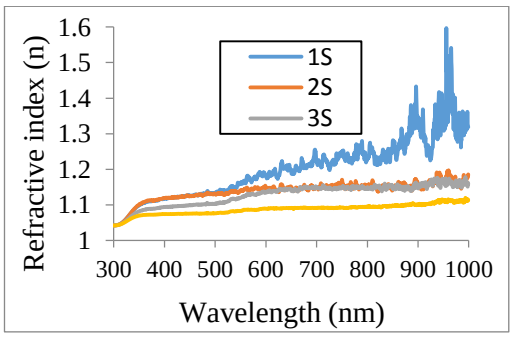


Figure 5: Plot of refractive index against wavelength for 1S, 2S, 3S and 4S.

The extent of energy absorption of a semiconductor is determined by the absorption coefficient of the material (Choudapura et al. 2019). The absorption coefficient, α associated with the strong absorption region of the film was determined from absorbance (%A) and the film thickness (t) using the relation (Balachander et al. 2016):

$$\alpha = \frac{2.303A}{t} \qquad (8).$$

The variations of absorption coefficients with photon energy for spin coated ZnS deposited at different number of spin time are represented in Figure 6. The absorption coefficients increase with increasing photon energy from 3.0 eV to 4.2 eV. Since ZnS belongs to the direct band gap semiconductor, the relationship between absorption coefficient (α) and incident photon energy (hυ) is represented in Figure 7 as (Antony et al. 2005):

$$(\alpha h\nu)^2 = A(h\nu - E_g) \qquad (9)$$

where: E_g is the optical energy band gap, while A is a constant that depends on the electronic transition probability. The band gap is determined by extrapolating the linear region near the onset, as shown in Figure 7.

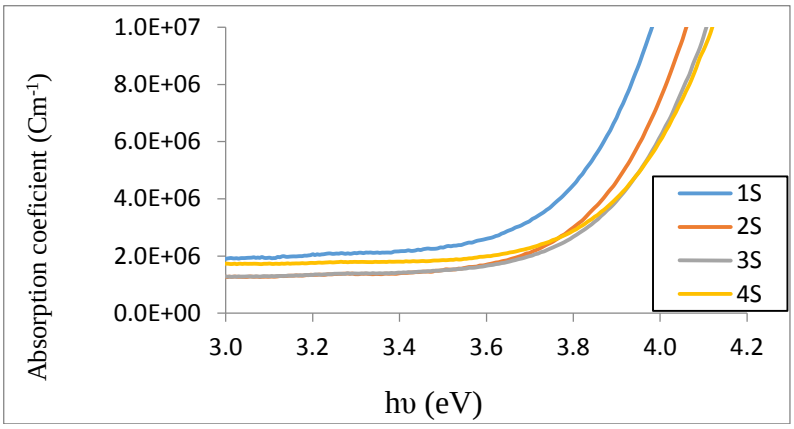


Figure 6: Plot of absorption coefficient against photon energy for 1S, 2S, 3S and 4S.

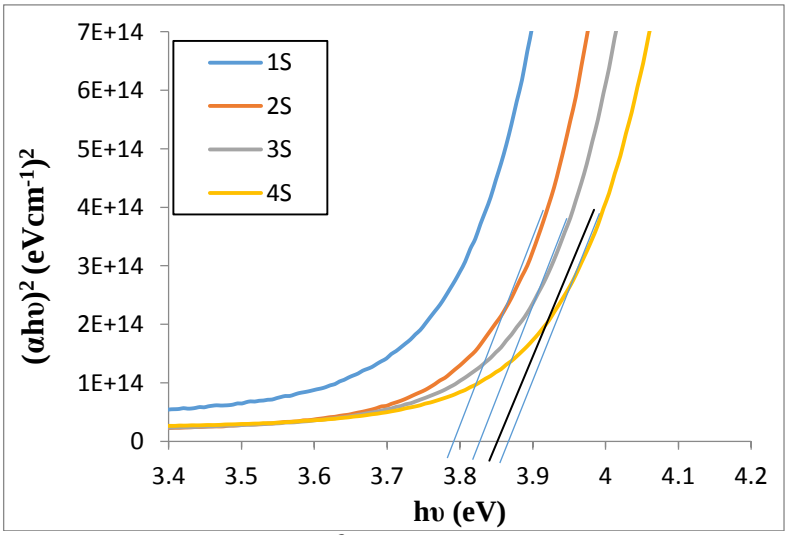


Figure 7: Plot of $(\alpha h\nu)^2$ against $h\nu$ for 1S, 2S, 3S and 4S.

The estimated values of energy band gaps for 1S, 2S, 3S and 4S are 3.70 eV, 3.80 eV, 3.84 eV and 3.87 eV, respectively. The literature reported value for band gap energy of bulk ZnS is 3.65 eV (Berger 1997). It is observed that the band gap values of the thin films from this study are higher than that of the bulk ZnS, indicating a shift in band gap energy which could be attributed to quantum confinement effects arising from lowering of particle sizes (Kalyanasundaram et al. 2013). These values of band gaps for ZnS are similar to the values reported in the literature. For example, Mukherjee and Mitra (2012) reported a band gap of 3.70 eV for ZnS thin films deposited by spin coating method at a spin speed of 4000 rpm for 60 seconds, while Zhou et al. (2013) reported a band gap of 3.70 eV for ZnS thin films deposited by chemical bath method. Manjulavalli and Kannan (2015) also reported values ranging between 3.84 and 3.96 eV for ZnS thin films deposited by chemical bath method. A range of band gap energy from 3.87 to 3.96 eV for chemical bath

deposited ZnS was also reported by Chabou et al. (2019). He attributed the increase in band gap with increasing deposition time to a decrease in the disorder as the films' thickness decreases. In particular, it is well known that the optical band gap of thin film materials, which are characterized by a length scale less than 10 nm, is higher than that of bulk material (Manjulavalli and Kannan 2015). It is also observed from Figure 8 that the energy band gap increases with increasing number of spin times.

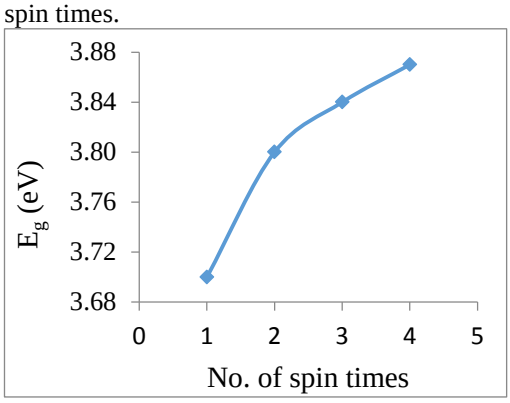


Fig. 8: Variation of bandgap of ZnS thin films with spin times.

The dielectric constant is related to refractive index (n) and extinction coefficient (k) by the relation (Ezema et al. 2007):

$$\varepsilon_r = n^2 - k^2 \quad (10)$$

for real part

and $\varepsilon_i = 2nk$ (11)

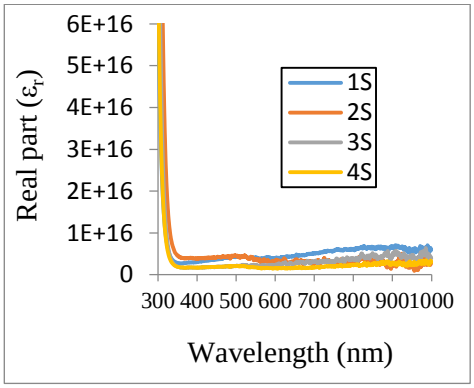
for imaginary part.

The plots of real (ε_r) and imaginary (ε_i) dielectric constant against wavelength are displayed in Figures 9 (a) and (b). Both real and imaginary dielectric constants decrease with increasing wavelength. They also show increase with increasing number of spin time.

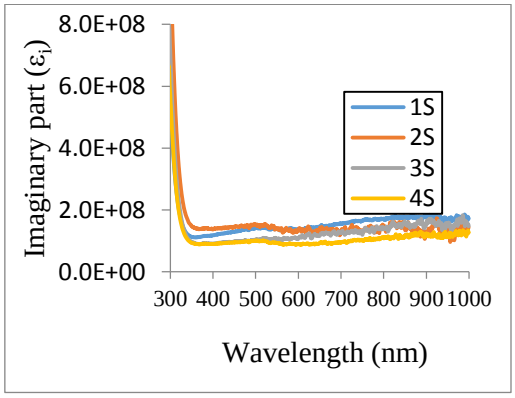
The absorption of the electromagnetic wave spectrum within thin films is dependent upon the material type, thickness, photo-conductivity, and extinction coefficient of the films (Hassanien and Akl 2015). The skin depth (χ), which is a phenomenon that describes the reduction in amplitude of electromagnetic wave after it has traversed a given thickness, has the formula (Abass 2015):

$$\chi = {}^{1}/_{\alpha} \quad (10)$$

where: α is the absorption coefficient.



(a)



(b)

Figure 9: Plot of (a) real and (b) imaginary part of dielectric constants against wavelength for 1S, 2S, 3S and 4S.

Figure 10 shows the dependence of skin depth on the photon wavelength (300 to 900 nm) for 1S, 2S, 3S and 4S. The skin depth increases as the wavelength increases up to the highest value of wavelength. It is also observed that as the number of spin times decreases, the skin depths decrease with the ZnS film deposited at three spin times (3S) showing the highest skin depth within the UV region of the wavelength. The 4S thin film deviated from the above trend as it showed the lowest value of skin depth.

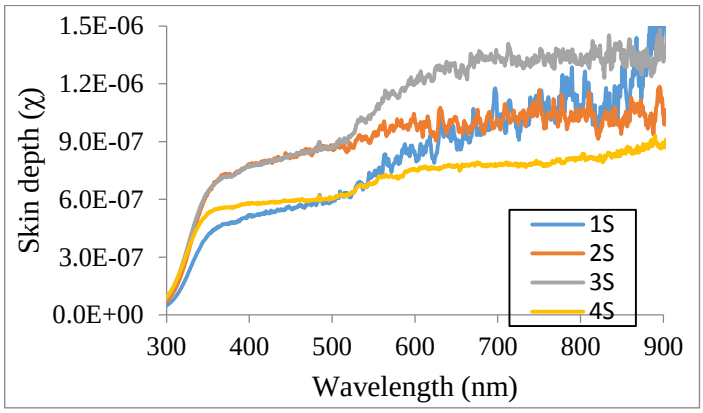


Figure 10: Plot of skin depth against wavelength for 1S, 2S, 3S and 4S.

Conclusion

Zinc sulphide thin films were prepared using spin coating method. The prepared films are polycrystalline in nature with cubic structure having reflections from (111), (220) and (311) planes. The broadening of the diffraction peak provides information about crystallite size. From the results of optical studies, it can be concluded that ZnS films exhibit good optical properties with relatively high transmittance (81%) and low absorbance (0.36 %) in the visible region. The increase in the number of spin time brings about a reduction in transmittance, dielectric constants, refractive index, extinction coefficient and absorption coefficient. The band gaps obtained range from 3.70 to 3.87 eV, which are above the energy band gap of the bulk ZnS (3.60) and the band gaps increase with increasing number of spin times. The morphology of the surface shows that the films are uniform throughout the surface. The EDX analyses revealed that zinc and sulphur are present in the films with 78.2% and 6.0% by weight, respectively. Therefore, the results of the study show that ZnS films can be a good candidate for optoelectronic devices especially in window layer of photovoltaic cells.

References

Abass HA 2015 Fe_2O_3 thin films prepared by spray pyrolysis technique and study the annealing on its optical properties. *Int. Lett. Chem. Phy. Astr.* 45: 24-31.

Abduljabbar LM 2014 Study the effect of annealing on optical and electrical properties of ZnS thin film prepared by CO2 laser deposition technique. *Iraqi J. Laser.* 13: 29-35.

Abdullah MT, Ahmad ASS, and Mohammed AA 2015 The effect of doped Indium on the electrical and optical properties of $(Se_{0.7}Te_{0.3})_{1-x}In_x$ thin films. *Adv. Mater. Phys. Chem.* 5: 140-149.

Akl AA, Mahmoud SA, Al-Shomar SM and Hassanien AS 2018 Improving microstructural properties and minimizing crystal imperfections of nanocrystalline Cu_2O thin films with different solution molarities for solar

application. *Mater. Sci. Semicond. Proc*. 74: 183-192.

Ali MM 2015 Effect of annealing temperature on the structural and optical properties of ZnS thin films deposited by CBD. *Basrah J. Sci. (A)*. 33(1): 156-181.

Antony A, Murali KV, Manoj R and Jayaraj MK 2005 The effect of the pH value on the growth and properties of chemical-bath deposited ZnS thin films. *Mater. Chem. Phy*. 90(1): 106–110.

Arandhara G, Saikia PK, and Bora J 2015 Optical and structural properties of ZnS thin films grown by chemical bath deposition technique using two different zinc salts. *J. Bas. Appl. Eng. Res.* 2(20): 1761-1764.

Bashar MS, Matin R, Sultana M, Siddika A, Rahaman M, Gafur MA and Ahmed F 2020 Effect of rapid thermal annealing on structural and optical properties of ZnS thin films fabricated by RF magnetron sputtering technique. *J. Theor. Appl. Phys.*14: 53-63.

Balachander M, Saroja M, Venkatalachalam M, Kumar V and Shankar S 2016 Structural and optical properties of zinc sulphide thin film prepared by sol-gel spin coating method. *Int. J. Chem Concepts* 2(2): 65-69.

Berger LI 1997 Semiconductor materials, CRC press, New York.

Banerjee R, Jayakrishnan R and Ayyub P 2000 Effect of the size-induced structural transformation on the band gap in CdS nanoparticles. *J. Phys. Condens. Matter* 12: 10647-10654.

Bendjedidi H, Attaf A, Saidi H, Aida MS, Semmari S, Bouhdjar A and Benkhetta Y 2015 Properties of n-type SnO_2 semiconductor prepared by spray ultrasonic technique for photovoltaic applications. *J. Semicond*. 36: 123002.

Chabou N, Birouk B, Aida MS and Raskin JP 2019 Deposition time and annealing effects on morphological and optical properties of ZnS thin films prepared by chemical bath deposition. *Mater. Sci.-Pol.* 37(3): 404-416.

ChoudapuraVH, Kapatkara SB and Rajub AB 2019 Structural and optoelectronic properties of zinc sulphide thin films synthesized by co-precipitation method. *Acta Chem. Iasi* 27(2): 287-302.

Dissanayake DMCU and Samarasekara P 2018 Effect of number of layers on structural and optical properties of spin coated CdS films. *J Sci.* 10: 13-20.

Eid AH, Salim SM, Sedik MB, Omar H, Dahy T and Abou-Elkhair HM 2010 Preparation and characterization of ZnS thin films. *J. Appl. Sci. Res.* 6(6): 777 784.

Elidrissi B, Addou M, Regragui M, Bougrine, Kachouane A and Bernede JC 2001 Structure, composition and optical properties of ZnS thin films prepared by spray pyrolysis. *Mater. Chem. Phys.* 68: 175-179.

Erken O, Gunes M, Ozaslan D and Gumus C 2017 Effect of the deposition time on optical and electrical properties of semiconductor ZnS thin films prepared by chemical bath deposition. *Indian J. Pure Appl. Phy.* 55: 471-477.

Ezema FI, Asogwa PU, Ekwealor ABC, Ugwuoke PE and Osuji RU 2007 Growth and optical properties of Ag_2S thin films deposited by chemical bath deposition technique. *J. Univ. Chem. Techn. Metall.* 42(2): 217-222.

Fukarova-Juruskovska M, Ristov M and Andonovski A 1997 Electroluminescent cell prepared by chemical deposition of ZnS:Mn thin film. *Thin Solid Films* 299(1-2): 149-151.

Gao XD, Li XM and Yu WD 2004 Morphology and optical properties of amorphous ZnS films deposited by ultrasonic-assisted successive ionic layer adsorption and reaction. *Thin Solid Films* 468: 43-47.

Hassanien, AS and Akl AA 2015 Influence of composition on optical and dispersion parameters of thermally evaporated non-

crystalline $Cd_{50}S_{50-x}Se_x$ thin films. *J Alloy Compd*. 648: 280–290.

Johnston DA, Carletto MH, Reddy KTR, Forbes I and Miles RW 2002 Chemical bath deposition of zinc sulfide based buffer layers using low toxicity materials. *Thin Solid Films* 404: 102-106.

Liu J, Wei A and Zhao Y 2014 Effect of different complexing agents on the properties of chemical-bath-deposited ZnS thin films. *J. Alloys Compd.* 588: 228–234.

Kalyanasundaram S, Panneerselvam K and Kumar VS 2013 Study on physical properties of ZnS thin films prepared by chemical bath deposition. *Asian Pac. J. Res.* 1(8): 1-7.

Kashani H 1996 Production and evaluation of ZnS thin films by the MOCVD technique as alpha-particle detectors. *Thin Solid Films* 288: 50-56.

Kavanagh Y and Cameron DC 2001 Zinc sulfide thin films produced by sulfidation of sol–gel deposited zinc oxide. *Thin Solid Films* 398–399: 24-28.

Kumar V, Saroja M, Venkatachalam M and Shankar S 2015 Synthesis and characterization of ZnS thin films by sol-gel dip and spin coating methods. *Int.. J. Rec. Sci. Res.* 6(11): 7377-7379.

Lindroos S, Kanniainen T and Leskela M 1994 Growth of ZnS thin films by liquid-phase atomic layer epitaxy (LPALE). *Appl. Surf. Sci.* 75: 70-74.

Mach R and Müller GO 1982 Physical concepts of high-field, thin–film electroluminescence devices. *Phys. Status Solidi* 69(1): 1-66.

Manjulavalli TE and Kannan AG 2015 Structural and optical properties of ZnS thin films prepared by chemical bath deposition method. *Int. J. ChemTech Res.* 8(11): 396-402.

Mukherjee A. and Mitra P 2012 Preparation of zinc sulphide thin film by spin coating and their characterization. *J. Phys. Sci.*16: 171-175.

Nasr TB, Kamoun N, Kanzari M and Bennaceur R 2006 Effects of pH on properties of ZnS thin films grown by chemical bath deposition. *Thin Solid Films* 500: 4–8.

Nair PK, Nair MTS, Garcia VM, Arenas OL, Pena Y, Castillo A, Ayala IT, Gomezdaza O, Sanchez A, Campos J, Hu H, Suarez R and Rincon ME 1998 Semiconductor thin films by chemical bath deposition for solar energy related applications. *Solar Energy Mater. Solar Cells.* 52: 313-344.

Nabiyouni G, Sahraei R, Toghiany M, Majles Ara MH and Hedayati K 2011 Preparation and characterization of nanostructured ZnS thin films grown on glass and n-type Si substrates using a new chemical bath deposition technique. *Rev. Adv. Mater. Sci*. 27: 52-57.

Nicolau YF 1985 Solution deposition of thin solid compound films by a successive ionic layer adsorption and reaction process. *Appl.. Surf. Sci*. 22-23:1061-1074.

Oladeji IO and Chow L 2005 Synthesis and processing of CdS/ZnS multilayer films for solar cell application. *Thin Solid Films* 474: 77-83.

Ortíz-Ramos, DE, González LA and Ramirez-Bon R 2014 p-Type transparent Cu doped ZnS thin films by the chemical bath deposition method. *Mater. Lett.* 124: 267-270.

Osiele OM 2001 Chemically Deposited ZnS thin film for solar energy applications. *J. Appl. Sci.* 4(1): 1690-1699.

Rahchamani SZ, Dizaji HR and Ehsani MH 2015 Study of structural and optical properties of ZnS zigzag nanostructured thin films. *Appl Surf. Sci*. 356: 1096-1104.

Rahimzadeh N, Ghodsi FE and Mazloom J 2018 Effects of starting precursor ratio on optoelectrical properties and blue emission of nanostructured C-ZnS thin films prepared by spin coating. *J. Electron. Mater*. 47: 1107-1116.

Roy R, Choudhary VS, Patra MK and Pandya A 2006 Effect of annealing temperature on the electrical and optical properties of nanocrystalline selenium thin films. *J. Optoelectron. Adv. Mater*. 8(4): 1352-1355.

Sartale SD, Sankapal BR, Lux-Steiner M and Ennaoui A 2005 Preparation of nanocrystalline ZnS by a new chemical bath deposition route. *Thin Solid Films* 480-481: 168-172.

Shaban M, Mustafa M, Hamdy 2015 Morphological and optical study of sol-gel spin coated nanostructured CdS thin films. *IOSR J. Appl. Phys.*7(6):19-22.

Shao LX, Chang KH and Hwang HL 2003 Zinc sulfide thin films deposited by RF reactive sputtering for photovoltaic applications, *Appl. Surf. Sci*. 212-213: 305-310.

Senthilarasu S, Sathyamoorthy R and Lalitha S 2004 Synthesis and characterization of β-$FeSi_2$ grown by thermal annealing of Fe/Si bilayers for photovoltaic applications. *Sol. Energy. Mater. Sol. Cells.* 82(1-2): 299-305.

Tec-Yam S, Rojas J, Rejón V, Oliva AI 2012 High quality antireflective ZnS thin films prepared by chemical bath deposition. *Mater. Chem. Phys.* 136: 386-393.

Tyona MD 2013 A theoretical study on spin coating technique. *Adv. Mater. Res.*. 2(4): 195-208.

Yano S, Schroeder R, Ullrich B and Sakai H 2003 Absorption and photocurrent properties of thin ZnS films formed by pulsed-laser deposition on quartz. *Thin Solid Films* 423: 273-276.

Zhou L, Tang N, Wu S 2013 Influence of deposition temperature on ZnS thin film performance with chemical bath deposition. *Surf. Coat. Technol.* 228: S146–S149.